JOURNAL OF AEROSPACE SOCIETY MALAYSIA

Volume 2, Issue 3

DECEMBER 2024

AEROSPACE SOCIETY MALAYSIA
PERSATUAN AEROANGKASA MALAYSIA
Registration No. PPM-001-10-09012017

Toward Greater Heights

JOURNAL OF AEROSPACE SOCIETY MALAYSIA

VOLUME 2, ISSUE 3
December 2024

eISSN 3009-0520

B-31-09, Kompleks EVO, Jalan Pusat Bandar 2, Seksyen 9,
43650 Bandar Baru Bangi, Selangor, Malaysia

Email: aeros_journal@aerosmalaysia.my

Journal of Aerospace Society Malaysia (AEROS Journal) is an open-access online journal that publishes high-quality research articles in all areas of aeronautics, astronautics and aviation. All submitted articles will undergo peer-review process before they are accepted for publication.

Publication Frequency: 3 times a year (end of April, August and December)

EDITORIAL

TABLE OF CONTENTS

JOURNAL OF AEROSPACE SOCIETY MALAYSIA

ARTICLE

FUEL BURN OPTIMISATION OF JET-PROPELLED AIRCRAFT DURING CLIMB USING EXCEL SOLVER

Khanin Aerpanich [1] and Siripong Atipan [1,*]

1. Department of Aerospace Engineering, Faculty of Engineering, Kasetsart University, 50 Ngamwongwan Rd, Chatuchak Bangkok 10900 Thailand

Correspondence: * siripong.a@ku.ac.th

Abstract: This research paper describes the creation and usage of a fuel burn optimization program for jet-propelled aircraft using Excel Solver. The main goal is to minimize fuel usage during the climb phase, thereby reducing the operational costs and environmental impact. The study uses a mathematical model incorporating various parameters from BADA (Base of Aircraft Data) to estimate the fuel consumption. Excel Solver is then utilized to find the best flight profiles such as airspeed and rate of climb to achieve the lowest possible fuel burn. The results show a significant reduction in fuel consumption across the different flight scenarios. The program's effectiveness has been validated through various case studies presented in this paper, which demonstrates improvements in fuel burn compared to traditional flight planning methods. The findings illustrate the practical benefits of integrating optimization tools into the aviation operations, leading to cost reduction and also supporting the goal of sustainable aviation by reducing greenhouse gas emissions. Additionally, this study includes recommendations for further refining the model to enhance accuracy and applicability.

Keywords: aircraft fuel optimization; climb optimization; aircraft fuel savings; Excel solver; jet aircraft

ABBREVIATION

BADA	: Base of Aircraft Data	MTOW	: Maximum Take-Off Weight
BADA OPF	: BADA Operation Performance File	TSFC	: Thrust Specific Fuel Consumption
BADA PTF	: BADA Performance Table File		

NOMENCLATURE

ρ	: Air density (kg/m^3)	η	: Thrust specific fuel flow (kg/min(kN))
C_D	: Drag coefficient	C_{D0}	: Zero-lift drag coefficient
C_{D2}	: Lift-induced drag coefficient	C_{fl}	: First TSFC coefficient
C_{f2}	: Second TSFC coefficient	C_L	: Lift coefficient
cTc	: Thrust constants	D	: Drag force (N)
dh/dt	: Vertical speed (m/s)	f_{cr}	: Cruise fuel flow (kg/min)
f_{nom}	: Nominal fuel flow (kg/min)	g	: Gravitational acceleration (m/s^2)
H_P	: Geopotential altitude (m or ft)	$KCAS$	: Calibrated air speed (knot)
m	: Aircraft mass (kg)	$T_{\max climb}$	: Maximum climb thrust (N)
T_{HR}	: Thrust acting parallel to the aircraft velocity vector (N)	T_{ratio}	: Ratio of applied thrust to maximum thrust
V_{TAS}	: True airspeed (m/s)	W	: Aircraft weight (N)

1. Introduction

In the contemporary era, the aviation sector faces a mounting pressure to enhance environmental sustainability. Climate change, which is primarily driven by the emissions of green-house gases including carbon dioxide, poses a significant global-threat. In 2016, the International Civil Aviation Organization (ICAO) implemented Carbon Offsetting and Reduction Scheme for International Aviation (CORSIA) as an Annex to the Chicago Convention, which all of ICAO's member states must apply from 2019 [1]. Hence it is important to find effective solutions to address this issue and one of them is the optimization of aircraft fuel-burn.

To date, many researchers have been working on reducing the aircraft's fuel consumption during different flight phases. For instance, Mori (2020) performed optimization of the cost function using the pseudo-spectra method by varying calibrated airspeed (CAS), altitude and thrust settings [2]. The result saved 85 lbs. or 0.51% over the period of climb from 10,000 ft to 30,000 ft and cruise to reach a distance of 300 nm. In the meantime, Zhang et al. (2019) studied the continuous climb operation of A320 from sea level to FL240 with constant angle of climb [3]. The result was then compared with the traditional procedure, which showed a 12.3% reduction in fuel consumption. Furthermore, a powerful method of multi-objective environmental optimization during the departure procedure using differential evolution algorithm is presented Ref. [4]. Moreover, Wan et al. (2020) applied multi-objective optimization with genetic algorithm to the climb phase of a Boeing 737-800 aircraft [5]. It is found that, for climbing flight from an altitude of 10,000 ft to 28,000 ft and a distance of 250 km, the fuel consumption can be reduced up to 6% with the optimized aircraft speed variation. Alexandrov et al. (2022) performed optimization by varying the thrust and pitch controls to achieve fuel cost within time constraints of an aircraft during climbing from 1,500 ft to 34,000 ft and within the distance of 250 km, resulting in up to 1.5% fuel consumption reduction using the gradient-free search method [6]. However, it should be noted that all of the previously mentioned algorithms are resource-intensive and time-consuming. Hence it is taught that, with a single-objective optimization problem, a simpler method like generalized reduced gradient (GRG) method may be applicable to find solutions with less time and resources.

This research studies on optimization of fuel consumption during climb of the Airbus A320 aircraft by varying calibrated airspeed, with a given initial speed at start altitude to a given final end airspeed at the required altitude and distance. The study delves into the development of Fuel-Burn Optimization Tool of a jet-propelled aircraft during climb using GRG nonlinear method available in the Excel-Solver Add-in to solve for the optimal calibrated airspeed variation and flight trajectory.

2. Methodology

The fuel consumption model and aircraft parameters for the Airbus A320 aircraft are taken from the Base of Aircraft Data (BADA) revision 3.8, with some mathematical derivatives of the model [7]. The aircraft aerodynamics and fuel consumption models during climbing phase are described as follows. Firstly, Equation 1 shows the total energy model.

$$(T_{HR} - D)V_{TAS} = mg\frac{dh}{dt} + mV_{TAS}\frac{dV_{TAS}}{dt} \tag{1}$$

During cruise flight phase, the energy model becomes Equation 2, where drag (D), drag coefficient (C_D) and lift coefficient (C_L) are calculated using Equation 3, Equation 4 and Equation 5, respectively.

$$T_{HR} = D + m\frac{dV_{TAS}}{dt} \tag{2}$$

$$D = \frac{W \cdot C_D}{C_L} \tag{3}$$

$$C_D = C_{D_0} + C_{D_2} \times C_L^2 \tag{4}$$

$$C_L = \frac{2W}{\rho V_{TAS}^2 S} \tag{5}$$

On the other hand, during climbing and accelerated flight, the applied thrust is defined in the form of thrust ratio as given in Equation 6 and Equation 7. Meanwhile, the rate of climb can be evaluated by Equation 8. Moreover, to obtain the time spent in flight, Equation 9 can be used.

$$T_{HR} = T_{ratio} \cdot T_{\max climb} \tag{6}$$

$$T_{\max climb} = C_{Tc,1} \times (1 - \frac{H_P}{C_{Tc,2}} + C_{Tc,3} \times H_P^2) \tag{7}$$

$$\frac{dh}{dt} = \frac{(T_{HR} - D)V_{TAS}}{mg} - \frac{V_{TAS} dV_{TAS}}{g dt} \tag{8}$$

$$dt = \frac{w}{(T_{HR} - D)V_{TAS}} dh + \frac{w}{(T_{HR} - D)g} dV_{TAS} \tag{9}$$

In the meantime, the fuel consumption rate can be evaluated by calculating the thrust specific fuel consumption (kg/min*kN), nominal fuel flow (which is valid in all phases except for the idle descent and cruise)(kg/min) and the cruise fuel flow (kg/min) as respectively given in Equation 10, Equation 11 and Equation 12.

$$\eta = C_{f1} \times (1 + \frac{V_{TAS}}{C_{f2}}) \tag{10}$$

$$f_{nom} = \eta \times T_{HR} \tag{11}$$

$$f_{cr} = \eta \times T_{HR} \times C_{fcr} \tag{12}$$

In addition, the numerical model for estimating the acceleration of aircraft is given as Equation 13. The Trapezoid Rule [9] is applied to obtain better estimates of the time in each climb step. By integrating both sides of previous Equation 9 results in Equation 14 and Equation 15.

$$\frac{dV_{TAS}}{dt} \approx \frac{\Delta V_{TAS}}{\Delta t} \tag{13}$$

$$\int_{t_{i-1}}^{t_i} dt = \int_{h_{i-1}}^{h_i} \frac{w}{(T - D)V_{TAS}} dh + \int_{V_{i-1}}^{V_i} \frac{w}{(T - D)g} dv \tag{14}$$

$$t_i - t_{i-1} = \frac{1}{2}\left[\frac{w_i}{(T_i - D_i)V_{TAS_i}} + \frac{w_{i-1}}{(T_{i-1} - D_{i-1})V_{TAS_{i-1}}}\right](h_i - h_{i-1}) + \frac{1}{2}\left[\frac{w_i}{(T_i - D_i)g} + \frac{w_{i-1}}{(T_{i-1} - D_{i-1})g}\right](V_{TAS_i} - V_{TAS_{i-1}}) \quad (15)$$

In this study, three different cases have been studied. All simulated flights begin with the aircraft's MTOW of 77,000 kg, climbing from 5,000 ft to 30,000 ft under the international standard atmosphere condition and with maximum climb thrust, and cruising to reach 300 km. The three studied cases are presented as follows.

Case-1: The aircraft climbs with 200 KCAS from 5,000 ft to 30,000 ft., accelerates with level flight to 280 KCAS which is the best range airspeed at altitude of 30,000 ft ISA, and then cruises until reaching the distance of 300 km.

Case-2: The aircraft accelerates with level flight from 200 to 280 KCAS, then climbs with 280 KCAS to 30,000 ft, and then cruises at 30,000 ft until reaching the distance of 300 km

Case-3: The aircraft climbs from 5,000 ft to 30,000 ft with optimized airspeed then cruises until reaching the distance of 300 km.

For this study, the optimization statement can be written as follows:

Minimize $\sum_{i=1}^{N} f_i \times (t_i - t_{i-1})$ (16)

with respect to

$V_{TAS} \in [V_{stall}, V_{max}]$ Velocity must be within flight envelope

$T_{HR} \in [0, T_{\max climb}]$ Thrust must not higher than maximum climb thrust

and subject to

$(t_i - t_{i-1}) > 0$ Time spent in each segment must be positive

where N represents the each segment of the altitude steps.

*Notes: While cruising, $f_i = f_{cr}$ and T_{HR} is a result from solving Equation 2, otherwise while climbing or accelerated flight, $f_i = f_{nom}$ and $T_{HR} = T_{\max climb}$ $(T_{ratio} = 1)$.

The computation process is presented as the flowchart in Figure 1. Each flight is simulated by the altitude step of 1,000 ft. In each step, the program computes the fuel flow using BADA model presented by previous Equation 1 to Equation 12. Meanwhile Equation 15 is used to compute the time. Then the total fuel consumption is calculated as accumulation of fuel mass from each step as per Equation 16. The optimization is done by varying the variable airspeed until the minimum fuel consumption is found. In this study, the Excel Solver, which is a built-in Microsoft Excel tool by Frontline Systems [8], is used for the optimization process. The Excel Solver can find an optimal (maximum or minimum) value for a formula in one cell (called the objective cell), subject to constraints or limits on the values of other formula cells on a worksheet by changing the variable cells. It has an option to solve linear, integer and non-linear problems. Due to the non-linear problem nature of the optimization in this study, the Excel Solver is set to multi-start with 1,000 starting points in hope of obtaining the global solution. In addition

to the above, a validation simulation of a flight is done using the parameters from BADA OPF and compared to the performance data from BADA PTF.

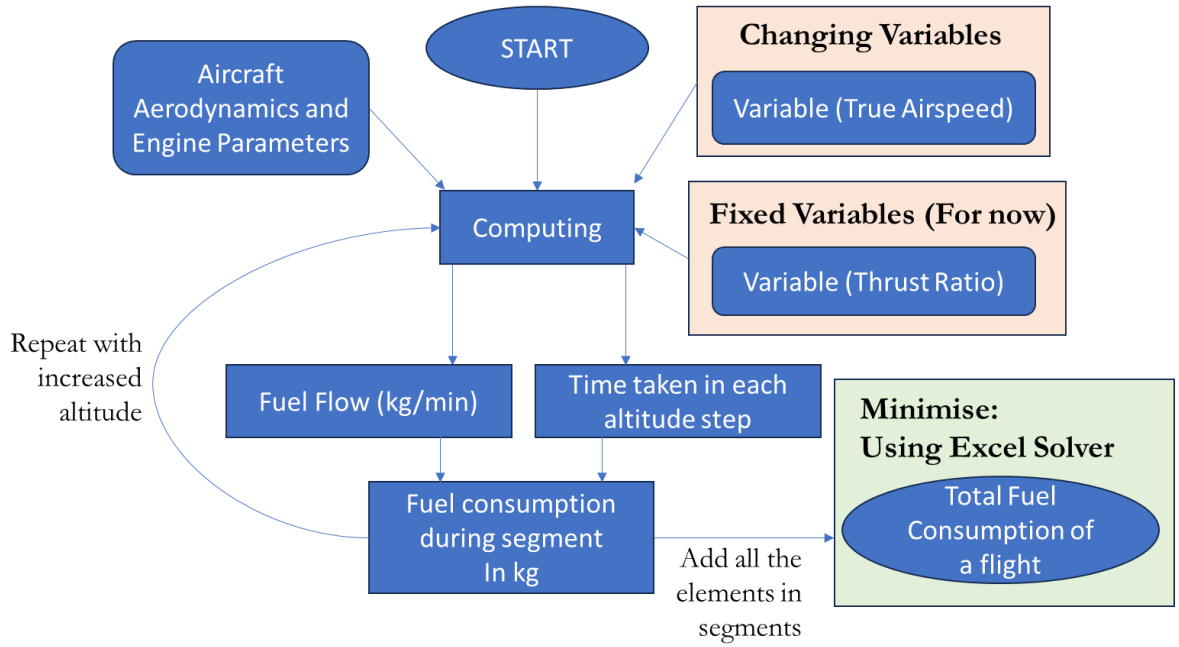

Figure 1: Flowchart describing the overall steps for this research study

In the Excel setup, each row of the spreadsheet represents the value of the respective parameters, and each column represents the simulation for each altitude ranging from 5,000 ft to 30,000 ft. This is shown in Figure 2. The steps in setting up the Excel spreadsheet are briefly described as follow:

Step 1 : Import aircraft's parameters $(S, CD_0, CD_2, T_{max,0}, cTc, c_f, V_{stall}, V_{max})$ from BADA OPF (Operation Performance file) to Excel. Note that since the parameter values are specifically requested from BADA, this step is kept confidential.

Step 2 : Calculate the International Standard Atmosphere parameters (ρ, P) for each altitude as per BADA User Manual [7].

Step 3 : Calculate the remaining parameters using equations from Section 1, Section 3 and BADA User Manual [7].

Step 4 : For Case 1 and 2, fill the assigned airspeed of each altitude step in Figure 2 (orange fill). On the other hand, for Case-3, open and set up the Solver Parameters Dialogue as in Figure 3. When recreating, set each box to reflect your work. In Figure 2, the orange fill represents the "Changing Variable" and the summation of the values in the green cell represents the "Objective".

Calculation							
Hp	5000	5000	6000	7000	8000	9000	10000
T	278.244	278.244	276.2628	274.2816	272.3004	270.3192	268.338
P	1760.7997	1760.799707	1695.895	1632.94173	1571.89401	1512.70762	1455.33883
rho	0.0020488	0.002048775	0.001987	0.00192745	0.0018689	0.00181171	0.00175587
P (Pa)	84307.265	84307.26454	81199.6	78185.3563	75262.3603	72428.4867	69681.6416
VCAS (knots)	200	200	200	200	200	200	200
VTAS (ft/s)	362.83584	362.8358404	368.2089	373.694138	379.294459	385.012738	390.85195
CL	0.9538331	0.953833147	0.954799	0.95524526	0.95573427	0.95626782	0.95684782
CD	0.0580273	0.058027268	0.058094	0.05812469	0.05815846	0.05819533	0.05823543
D	10327.077	10327.07651	10328.47	10323.0492	10317.6703	10312.3388	10307.0533
Tmax,climb	28512.819	28512.81859	27887.42	27266.1357	26648.9765	26035.9388	25427.0225
T/Tmax	1	1	1	1	1	1	1
T	28512.819	28512.81859	27887.42	27266.1357	26648.9765	26035.9388	25427.0225
dt new		0	27.57756	28.2029172	28.8584425	29.5618022	30.3181323
V TAS (kt)		214.9756134	218.1591	221.409016	224.727135	228.115143	231.574801
eta		0.791785799	0.794133	0.79652868	0.79897488	0.80147261	0.80402317
fuel flow		95525.14456	98511.22	96607.1598	94710.4646	92820.9982	90938.6234
fuel	0	0	45.27832	45.4100622	45.553275	45.7325997	45.9514869
fue acc	0	0	45.27832	90.6883811	136.241656	181.974256	227.925743
time acc	0	0	27.57756	55.7804788	84.6389213	114.200723	144.518856
d acc (km)	0	0	3.117613	6.35355769	9.71448232	13.2093776	16.8482074

Figure 2: Calculation table for Step 2 and Step 3 (taken partially from 5,000 ft to 10,000 ft)

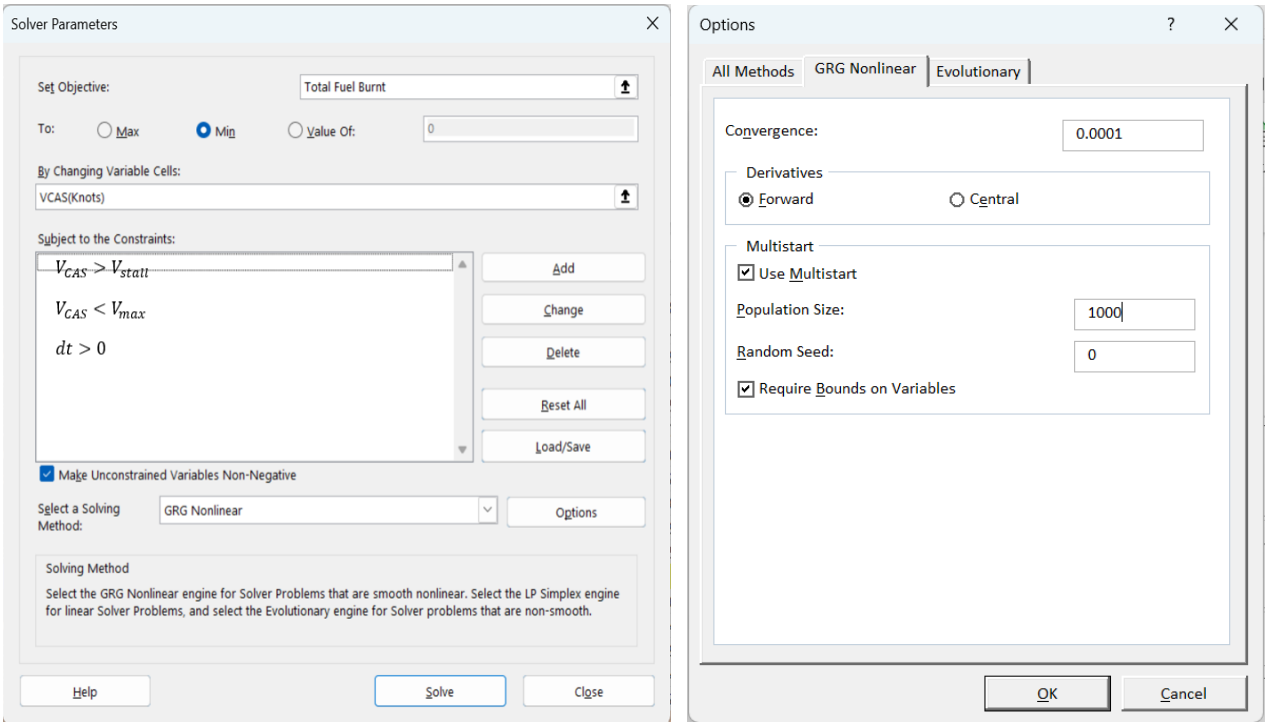

Figure 3: Solver parameters dialogue set-up

3. Results and Discussion

In the first part of the study, the performance model is validated with the performance data from BADA PTF (BADA PTG dated 01 Apr 2010). The comparison of the results is shown in Figure 4. As

can be observed, the result using the present model agrees well with the reference model with a mean absolute error (MAE) of 0.0377 kg/min or a mean absolute percentage error (MAPE) of 0.02%.

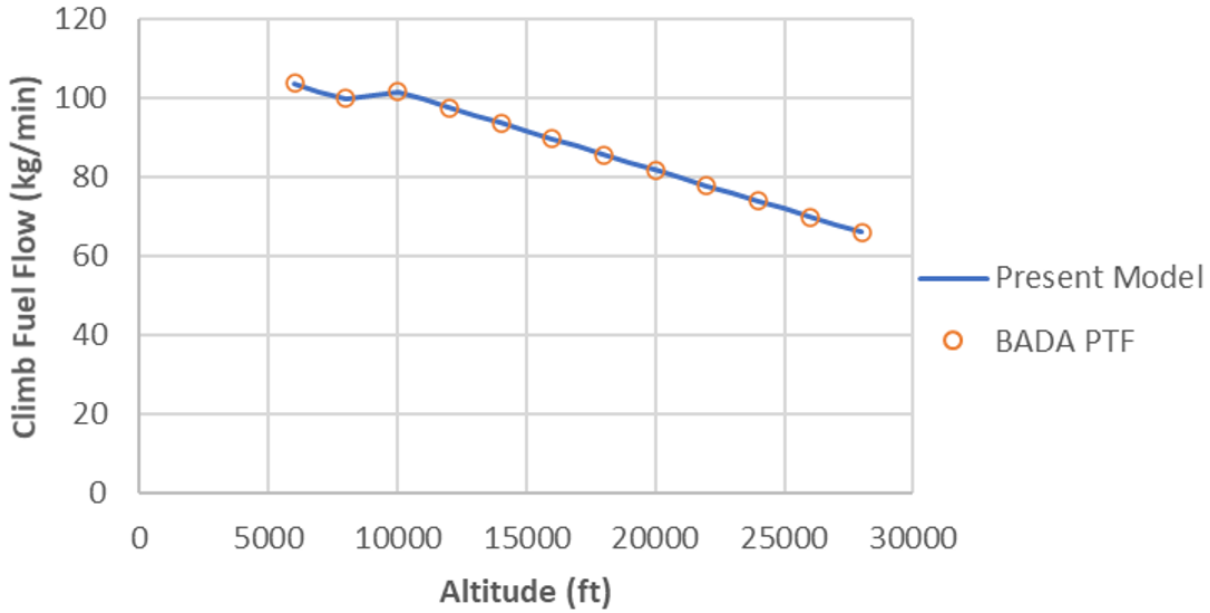

Figure 4: Validation of climb fuel flow

In the simulation of Case-1, the flight begins with climbing from 5,000 ft at constant KCAS of 200 knots up to 30,000 ft, then accelerating with level flight to 280 KCAS, and cruising until reaching the distance of 300 km. Computation of aerodynamics-based BADA model then provides the true airspeed, rate of climb, duration to climb and cruise, distance and the amount of fuel used until completing the flight. The true airspeed profile and altitude flight trajectory are illustrated in Figure 5. The calculation provides the total fuel burn of 1915.3 kg.

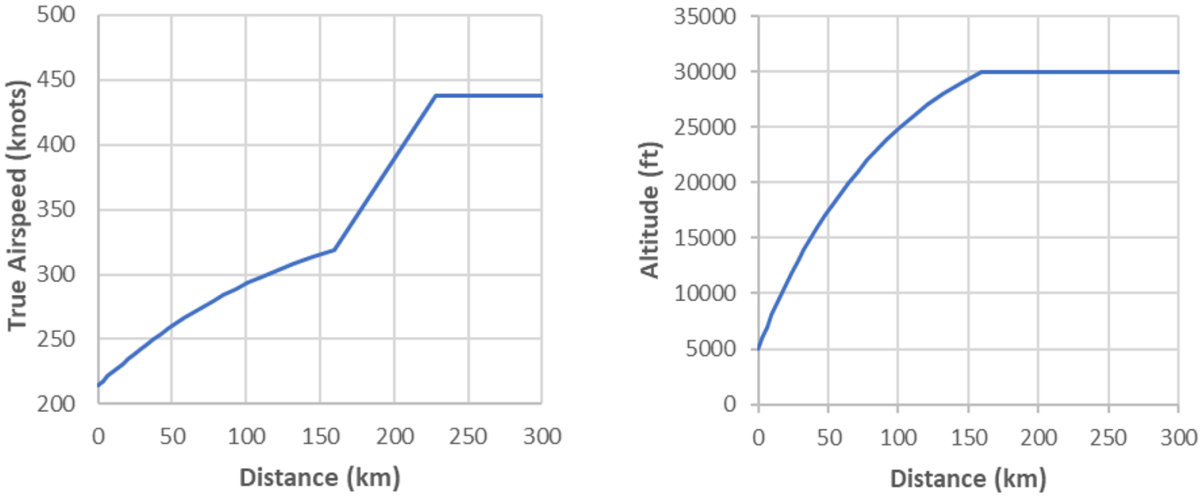

(a) True airspeed profile (b) Flight trajectory

Figure 5: True airspeed profile and flight trajectory of Case-1

In the simulation of Case-2, the flight begins with accelerating from CAS of 200 knots to 280 knots at an altitude of 5,000 ft, then climbing to 30,000 ft with constant CAS of 280 knots, and cruising until

reaching the distance of 300 km. The computation provides the true airspeed profile and flight trajectory as shown in Figure 6. The calculation provides the results of total fuel burn as 1699.5 kg.

Last but not the least, in the simulation of Case-3, the flight begins with accelerating from CAS of 200 knots to the optimized airspeed at altitude of 5,000 ft, then climbing to 30,000 ft with the optimized airspeed, and cruising until reaching the distance of 300 km. The optimized speed is determined using the Excel Solver. The computation provides the true airspeed profile and flight trajectory as shown in Figure 7. The calculation provides the results of total fuel burn as 1689.3 kg.

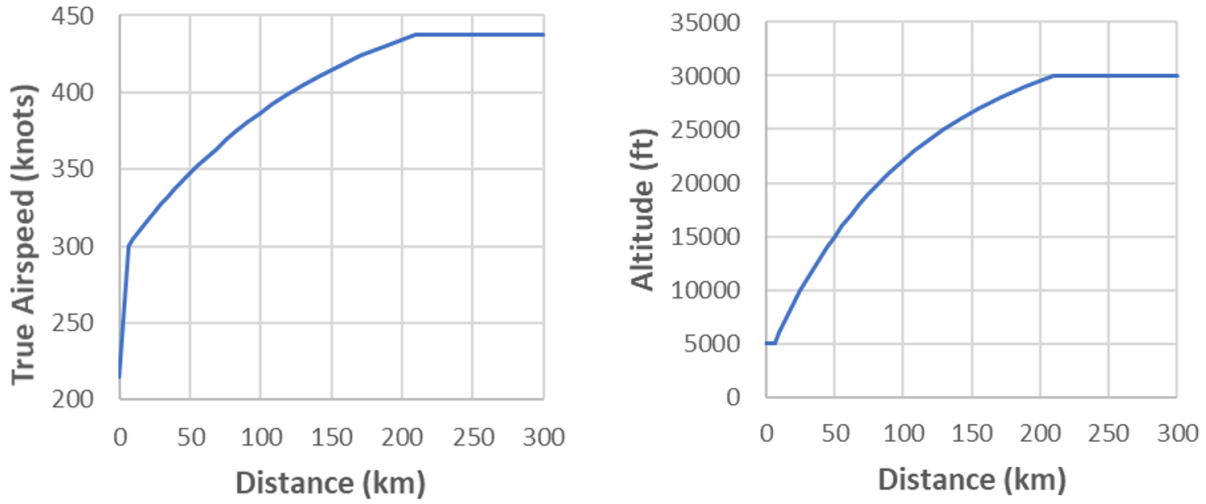

(a) True airspeed profile (b) Flight trajectory

Figure 6: True airspeed profile and flight trajectory of Case-2

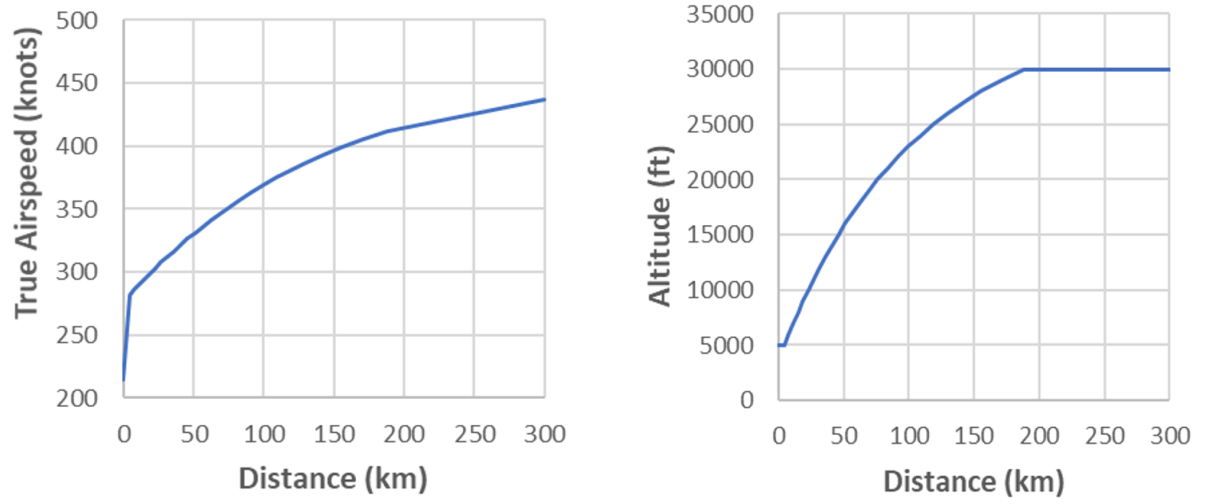

(a) True airspeed profile (b) Flight trajectory

Figure 7: True airspeed profile and flight trajectory of Case-3

From the case studies mentioned above, the optimization of airspeed (Case-3) has been shown to help reduce the fuel burn by 226 kg when compared to Case-1 and 10.2 kg when compared to Case-2. Nevertheless, the amount saved from Case-2 is minimal due to climb calibrated airspeeds are constant and similar to Case-2 during the climb phase. Figure 8 compares the trajectory of the different cases.

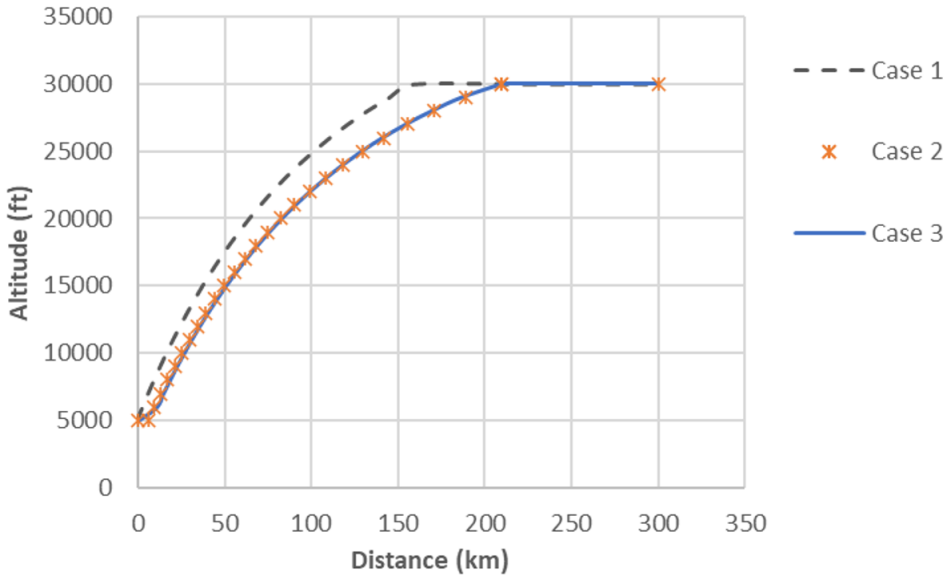

Figure 8: Flight trajectories of different cases

4. Conclusion

In this study, a fuel burn optimization program has been created and used for jet-propelled aircraft using Excel Solver. The objective is to minimize the fuel usage during the climb phase, thereby reducing the operational costs and also environmental impact. Based on obtained results, a significant reduction in fuel consumption across the different flight scenarios has been demonstrated using the optimization program. Nevertheless, there are some limitations in this study that may need to be addressed in further research. Firstly, the model has not yet involved the flight envelope into consideration. Secondly, the model utilizes the International Standard Atmospheric conditions. Further upgrade to the model can be achieved to accommodate non-standard conditions. Finally, further research on optimized variable airspeed and thrust during climbing and accelerating should be considered.

Acknowledgement

This study has been funded by the Master's Degree Education Promotion Program, Plan A, Faculty of Engineering, Kasetsart University, Thailand.

References

[1] IATA. (2024). CORSIA Fact Sheet. Retrieved from https://www.iata.org
[2] R. Mori, 'Fuel-Saving Climb Procedure by Reduced Thrust near Top of Climb', Journal of Aircraft, vol. 57, no. 5, pp. 800-806, 2020.
[3] M. Zhang, Q. Huang, S. Liu and Y. Zhang, 'Fuel Consumption Model of the Climbing Phase of Departure Aircraft Based on Flight Data Analysis', Sustainability, vol. 11, no. 16, 2019.
[4] Q. McEnteggart and J. F. Whidborne, 'Multiobjective Environmental Departure Procedure Optimization', Journal of Aircraft, vol. 55, no. 3, pp. 905-917, 2018.
[5] J. Wan, H. Zhang, F. Liu, W. Lv and Y. Zhao, 'Optimization of Aircraft Climb Trajectory considering Environmental Impact under RTA Constraints'. Journal of Advanced Transportation, vol. 2020, pp. 1-17, 2020.

[6] V. A. Alexandrov, E. Y. Zybin, V. V. Kosyanchuk, N. I. Selvesyuk, A. A. Tremba and M. V. Khlebnikov, 'Optimization of Aircraft Fuel Consumption During the Climb Phase', Automation and Remote Control, vol. 83, pp. 1742-1757, 2022.

[7] EUROCONTROL, User Manual for Base of Aircraft Data (BADA) Revision 3.8 (2010-003), 2010.

[8] Microsoft Support. Define and Solve a Problem by Using Solver. Retrieved from https://support.microsoft.com

[9] R. Johnsonbaugh, 'The Trapezoid Rule, Stirling's Formula and Euler's Constant', The American Mathematical Monthly, vol. 88, no. 9, pp. 696-698, 1981.

JOURNAL OF AEROSPACE SOCIETY MALAYSIA

ARTICLE

AERODYNAMIC CHARACTERIZATION AND MISSION PERFORMANCE ANALYSIS OF A LIGHT SEAPLANE DESIGN

Marwan Mohamed Magdi [1,*], Ezanee Gires [1,2,], Azmin Shakrine Mohd Rafie [1], Syaril Azrad Md Ali [1], Amzari Zhahir [1] and Mohd Faisal Abdul Hamid [1]**

1. Department of of Aerospace Engineering, Faculty of Engineering, Universiti Putra Malaysia, 43400 Serdang, Selangor, Malaysia
2. Aerospace Malaysia Research Centre (AMRC), Faculty of Engineering, Universiti Putra Malaysia, 43400 Serdang, Selangor, Malaysia

Correspondence: * marwanmagdi@proton.me, ** ezanee@upm.edu.my

Abstract: This paper presents the modeling, aerodynamic characterization and mission performance analysis of a seaplane design that is based on the AeroVolga Borey, utilizing a baseline Rotax 912 ULS engine configuration. The seaplane, with its amphibious capabilities, plays a critical role in connecting remote regions, yet detailed aerodynamic analyses of such aircraft are scarce. This study aims to address the gaps by focusing on the seaplane's aerodynamic properties and mission performance. A 3D-printed model of the Borey seaplane was tested in an open-loop wind tunnel, providing lift and drag coefficients under various flight conditions. From the experimental results, the highest lift-to-drag ratio was found to be 8.9. The aerodynamic data were then integrated into a mission performance simulation to assess its fuel burn, range and performance in different flight phases. On the whole, the study finds that the resultant aerodynamic and mission performance characteristics are aligned closely with the benchmark design data, highlighting the Borey's big potential as a short-to-medium-range seaplane. The maximum range calculated is 685 km, with error of 7.4% relative to the design specification. Findings from this study further contribute to a better understanding of seaplane performance, with practical applications for seaplane design and mission planning.

Keywords: aircraft performance; seaplane; aerodynamics; propulsion; mission analysis

1. Introduction

Seaplanes serve a unique role in aviation by combining both maritime and aerial capabilities, making them essential for connecting remote and also water-abundant regions. The Borey seaplane is a single-engine, amphibious aircraft that is capable of operating from both land and also water. It has an empty weight of 350 kg, a maximum weight of 650 kg, and a take-off distance of 350 meters on land and 450 meters on water [1]. Despite their importance, seaplanes remain essentially underexplored in terms of detailed aerodynamic analysis. Previous researches on seaplanes frequently highlights the challenges of balancing hydrodynamic and aerodynamic performance, particularly with regards to the drag penalties imposed by water operations [2]-[3]. However, there are also studies that provide a detailed exploration of the aerodynamic performance of amphibious aircraft including the Borey. This study addresses that gap by examining the aerodynamic properties and mission performance of the Borey using wind tunnel data and mission simulations.

Seaplanes have gained renewed interest due to their unique capability to operate in remote, water-centric regions, supporting activities such as marine tourism, transport and environmental monitoring.

A study on the seaplane operations in Gili Iyang, Indonesia, highlights their role in advancing the marine tourism and regional connectivity, emphasizing the importance of strategic deployment for sustainable economic growth [4]. In terms of market trends, amphibious aircraft have shown a steady increase in demand within civil aviation, particularly in areas requiring versatile access where traditional runways are unavailable. This growing demand aligns with broader transportation trends toward more flexible, multi-purpose aviation solutions. Regarding future technologies, the shift towards more electrification and hybrid power systems is pivotal for greener seaplane operations. The hybrid powertrains are being explored to reduce emissions and improve fuel efficiency, which is particularly relevant in the aviation sector's drive for higher sustainability. A comprehensive review of powertrain electrification strategies emphasizes that hybrid and electric engines could reduce greenhouse gas emissions and noise pollution, making them ideal for sensitive and eco-conscious regions [5]. Furthermore, with the advancements in autonomous flight technology, there is a great potential for seaplanes to be employed in many persistent, unmanned missions, further extending their operational capabilities in various industries.

The Borey seaplane, equipped with a Rotax 912 ULS engine, offers an ideal platform for studying the interaction between aerodynamics and mission performance in amphibious aircraft. This study seeks to provide comprehensive insights into the aerodynamic behavior of the Borey seaplane, as shown in Figure 1, with the focus on how its design and engine configuration influence its mission performance, including fuel consumption and also operational range. The primary goal is to analyze the aerodynamic performance and mission capabilities of the Borey seaplane using its baseline Rotax 912 ULS engine configuration. Findings from this study will contribute to the efforts in optimizing seaplane design and improving its operational efficiency. The detailed aerodynamic data can help in refining lift and drag characteristics while the mission analysis can offer practical insights into the fuel consumption patterns. This research might also serve as the foundation for future studies in exploring alternative powerplant configurations such as hybrid or electric propulsion systems.

Figure 1: Borey Aircraft [6]

2. Methodology

In short, this study gathered aerodynamic data through wind tunnel testing of a 3D-printed model to accurately characterize the aerodynamic properties of the aircraft. Following this, a simulation model was developed to integrate both the aerodynamic and engine performance data. Using this model, the mission performance was analyzed, focusing on key parameters such as fuel burn and range estimation across different flight phases. These phases were evaluated to provide insights into the efficiency and endurance of the aircraft under several different operational conditions. Detailed description on the methodology that was followed in this study is presented in the following sections.

2.1. Aerodynamic data acquisition

The process of aerodynamic data acquisition started with the detailed preparation of a scaled model of the Borey seaplane using computer-aided design (CAD) software, SolidWorks. The model was based on dimensionless sketches with a careful attention given to maintaining the aircraft's proportions and aerodynamic features as closely as possible to the actual Borey seaplane. This included replicating key design features such as the transition from the keel to the tail and also integration of accurate fuselage dimensions. Challenges arose in capturing the complex curves, which required iterative adjustments to achieve a balance between model accuracy and structural stability. The 3D model was then divided into multiple parts, which were later 3D printed using a Creality CR-10 printer with 50% infill. This structural integrity was essential to ensure that the model could withstand the forces it would encounter during the experimental wind tunnel testing. The assembly of the parts was achieved using carbon rods as the reinforcements within the wings, providing additional support while preserving aerodynamic fidelity. The transposing of the 2D drawings to 3D representation is depicted in Figure 2. Table 1 and Table 2 list the geometric and also airfoil data used as reference in the CAD model and the scaled down version, respectively. Based on the shape of the airfoil, the reference airfoil is assumed to be Clark-Y type.

Figure 2: Constructed CAD model of the Borey seaplane

Table 1: Reference data used for the CAD modelling

Parameter	Value	Description
Airfoil Type	Clark-Y	Commonly used, flat-bottom airfoil
Chord Length	1.48 m	Distance from leading to trailing edge
Thickness-to-Chord Ratio	11.70%	Airfoil thickness as a percentage of chord length
Camber	3.40%	Maximum camber as a percentage of chord length, at 40% of chord
Leading Edge Radius	Approximately 0.04 - 0.05 m	Leading edge rounded radius (varies slightly with chord)
Wing Area	10 m^2	Total surface area of the aircraft wing
Span	9.76 m	Measurement of the wing's width from tip to tip

Table 2: Reference data used for the 3D model construction

Parameter	Value	Description
Airfoil Type	Clark-Y	Commonly used, flat-bottom airfoil
Chord Length	0.105 m	Distance from leading to trailing edge
Thickness-to-Chord Ratio	11.70%	Airfoil thickness as a percentage of chord length
Camber	3.40%	Maximum camber as a percentage of chord length, at 40% of chord
Leading Edge Radius	Approximately 0.00284 – 0.00355m	Leading edge rounded radius (varies slightly with chord)
Wing Area	0.71 m^2	Total surface area of the aircraft wing
Span	0.69 m	Measurement of the wing's width from tip to tip

To fit into the Universiti Putra Malaysia (UPM) Low-Speed Wind Tunnel testing area, the model was scaled down to about 7.1% of its original size, allowing it to conform to the wind tunnel's spatial constraints. Therefore, the wingspan of the wind tunnel model is 0.69 m. Figure 3 shows the 3D printer design files in addition to the printed parts. The pieces were then attached together using epoxy resin adhesive. Once assembled, the model's surface underwent intense smoothing using sandpaper, moving from coarse to fine grit to achieve a seamless finish. A primer layer was subsequently applied to highlight any imperfections, followed by a white paint coat, which served a dual purpose of aesthetics and also aerodynamics. Finally, a layer of wax was applied to reduce the skin friction drag. The final assembled model is shown in Figure 4.

The UPM Low-Speed Wind Tunnel was used to simulate various airflow conditions around the Borey aircraft model. The model was mounted within the test section using three metal rods connected to a six-axis component, allowing for precision adjustments of the angle of attack (AoA), which ranged from -9° to +15°. The wind tunnel was operated at airspeeds from 3 m/s up to 21 m/s, allowing for a comprehensive analysis of lift and drag forces across different flight scenarios. The installed model in the wind tunnel test section is depicted in Figure 5. At each angle of attack, the forces acting on the model, i.e. side force, drag and lift (F_x, F_y , F_z), in addition to roll, pitch and yaw moments were measured using a six-component balance. These measurements were used to derive the drag and lift coefficients. A secondary test was performed exclusively on the rods and plates that held the model in place. This allowed for the calculation of interference forces, which were then taken into account when calculating the drag coefficient.

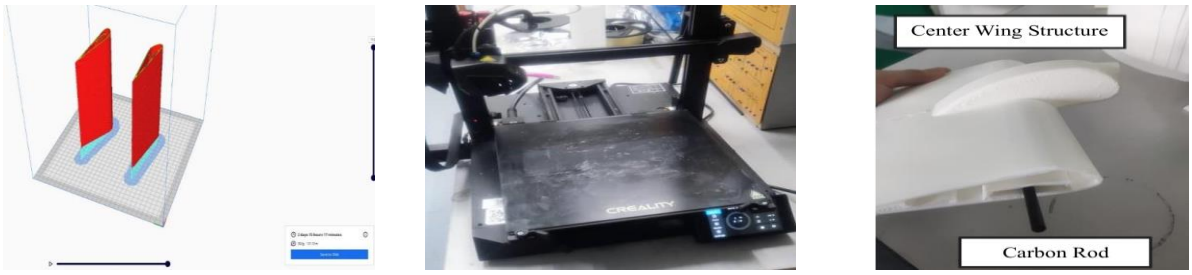

(a) Sliced parts (b) Creality CR-10 3D Printer (c) Carbon rods in the wing

Figure 3: Fabrication process of the model

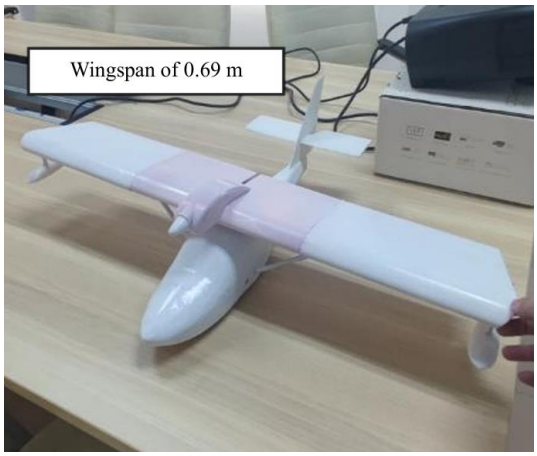

Figure 4: Final assembled model

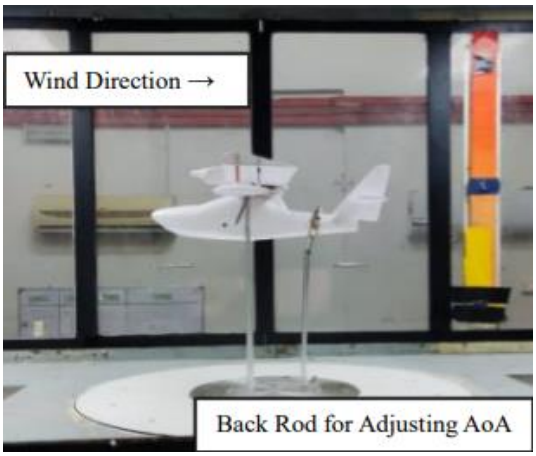

Figure 5: Strapped model in the wind tunnel

The lift and drag coefficients were calculated using Equation 1 and Equation 2, respectively, where ρ is density of air (kg/m³), v is velocity of the aircraft (m/s), S is wetted upper area of the aircraft (m²), C_L is coefficient of lift, $C_D$is coefficient of drag, L is lift force (N) and D is drag force (N).

$$C_L = \frac{L}{\frac{1}{2}\rho V^2 S_W} \tag{1}$$

$$C_D = \frac{D}{\frac{1}{2}\rho V^2 S_W} \tag{2}$$

2.2. Mission performance simulation

The mission simulation began with geographical data collection from Google Earth. Waypoints along the intended flight path were selected, including take-off, climb, cruise and descent points. Each waypoint's latitude and longitude were recorded to provide an accurate representation of the flight path and support the waypoint-based mission analysis. The waypoint-based analysis involved mapping out each flight phase along the path, with each waypoint acting as a node for analyzing performance metrics such as altitude, speed and also fuel consumption. These parameters were updated dynamically in the simulation model as the Borey aircraft transitioned from one waypoint to the next. Figure 6 shows the regional mission area (Peninsular Malaysia – Sumatera) used for the analysis.

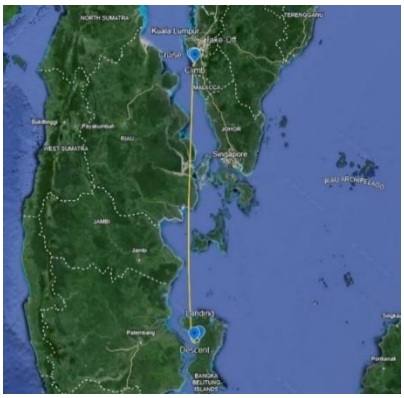

Figure 6: Geographic mission area

2.3. Fuel burn estimation

Fuel burn was calculated using available data in the Rotax 912 ULS engine manual. The correlation of shaft power to specific fuel consumption is obtained from publicly available engine data for Rotax 912S engine [7] and this is shown in Figure 7.

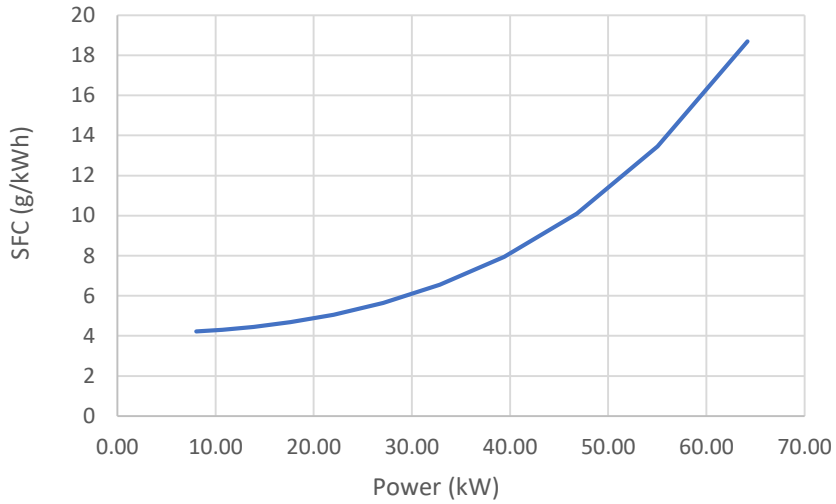

Figure 7: Power vs SFC

Certain power settings were used for the specific phases: take-off occurred at 100% power (which corresponds to 100 hp), cruise at 75% power and adjustments were made for other phases. Water drag forces were also factored into fuel consumption during water-based take-offs, using the drag equation for water to account for the extra power needed as in Equation 3, where F_D is drag force of water (N), ρ is density of water (kg/m^3), A is the lower wetted area (m^2) and C_{dw} is drag coefficient of water.

$$F_D = \frac{1}{2}\rho A v^2 C_{dw} \tag{3}$$

Summing the calculated fuel burn at each phase, the total fuel consumption for the entire mission was derived, giving a realistic assessment of operational efficiency under various loads and conditions. The Breguet Range Equation was then applied to determine the Borey's maximum range, as shown by Equation 4, using the lift-to-drag ratio from wind tunnel data and specific fuel consumption at cruise. In this equation, R is range (km), η_{pr} is propeller efficiency, SFC is specific fuel consumption (g/kWh), C_L is lift coefficient, C_D is drag coefficient, w_0 is gross mass (kg) and w_1 is empty weight (kg).

$$R = \frac{\eta_{pr}}{SFC}\frac{C_L}{C_D}\ln\left(\frac{w_0}{w_1}\right) \tag{4}$$

The propeller efficiency of the seaplane is calculated to be 70% using Equation 5, where η_{pr} is propeller efficiency, u_e is exit velocity (m/s) and u_0 is velocity of the aircraft (m/s). The design range of the aircraft is 740 km or 400 nm at cruise speed of 70 knots. The analysis was done for both no-payload and maximum-payload conditions to illustrate how weight and fuel load impacted the Borey's operational limits.

$$\eta_{pr} = \frac{2}{1 + \frac{u_e}{u_0}} \tag{5}$$

3. Results and Discussion

3.1 Aerodynamic characterization

From the wind tunnel testing, the graphs of lift and drag coefficients and versus angle of attack are shown in Figure 8 after accounting for interference such as the rods where another test was performed only on the rods then subtracted the results of the lift and drag coefficients respectively from the original result. As could be seen in Figure 8, lift increased proportionally with speed and angle of attack up to a certain point. The maximum lift coefficient, C_L was observed at an angle of approximately 10°, beyond which the lift force started to decrease as the model approached the stall condition. Correspondingly, drag coefficient, C_D increased as the angle of attack rose, reflecting the expected increase in resistance due to higher aerodynamic forces. At low angles of attack, the drag remained minimal, contributing to efficient cruise performance whereas higher angles resulted in sharp increases in drag. To quantify the efficiency of the model, the kift-to-drag (L/D) ratio was calculated for each test condition. The L/D ratio reached its peak at an angle of attack of 3°, indicating an optimal aerodynamic configuration for cruising. This peak L/D ratio of 8.9 can be taken to suggest that the Borey aircraft is most efficient in terms of lift versus drag at low angles of attack, making it suitable for steady cruise performance under standard mission conditions. Further validation was performed by comparing wind tunnel results with the simulation outputs from MachUp (Utah State University, 2024.). Figure 9 presents the lift and drag coefficients, which has similar results as the original wind tunnel test. Therefore, the wind tunnel test results were used for this paper.

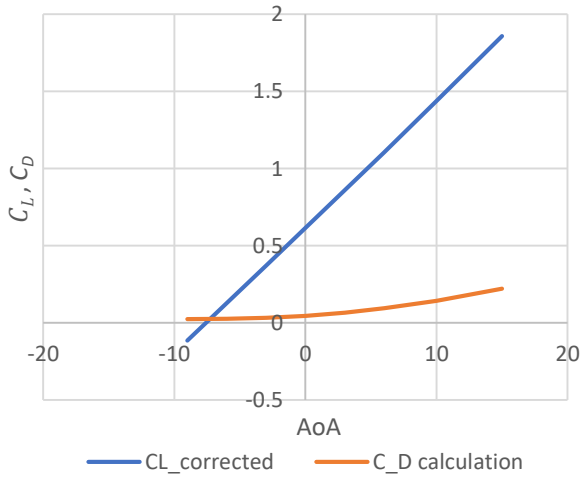

Figure 8: C_L and C_D versus AoA

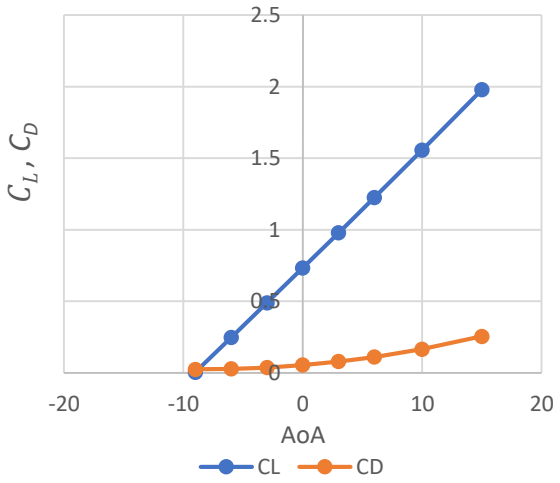

Figure 9: C_L and C_D in MashUp results

Based on the experimental data obtained, the plots for lift and drag of the aircraft versus speed are shown in Figure 10. With maximum all up mass of 650 kg, the minimum velocity for lift is 40 knots while the highest is 43 knots. The power curve for the aircraft is shown in Figure 10, where it could be seen that the maximum speed attainable by the seaplane is at 90 knots at 100% engine shaft power. The power in kilowatt calculated was by multiplying 0.001 with the drag in Newton and the respective speed in m/s. The RPM and the specific fuel consumption or the SFC were obtained using regression analysis as illustrated in Figure 11. Using curve fitting function in Microsoft Excel, it calculates the best-fit values by minimizing the difference between the actual data points and the fitted curve. The quality of the fit

is measured using the coefficient of determination, R^2. An R^2 value close to 1 indicates that the fitted curve explains 46 most of the variability in the data. In this study, the resulting equation from the curve fitting is SFC $=5 * 10^{-8} \cdot RPM$ 2.3239. This equation is derived from regression analysis and represents the relationship between SFC and RPM for the data set. This is a practical method to predict the SFC with different RPMs.

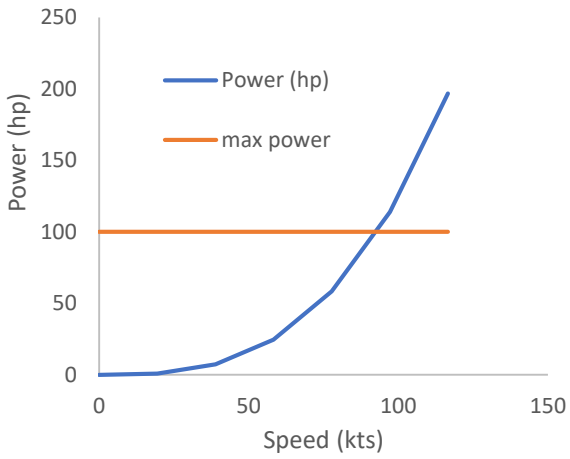

Figure 10: Power versus speed

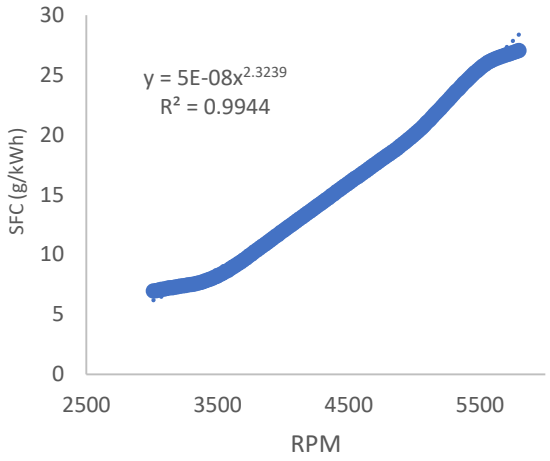

Figure 11: RPM versus SFC

As indicated in Figure 12, at lower speeds with 0° angle of attack, lift is lower than weight and this indicates insufficient lift to sustain the flight. As the speed increases, lift also begins to equal the weight, indicating that the aircraft can start to take off. As confirmed with Figure 12, the intersection points of both the weight and the lift where climb can occur, changes depending on the angle of attack. The lift at 12° angle of attack with 100 hp at 5800 RPM is 7994.81 N and the maximum weight for the aircraft is 650 kg multiplied by 9.81 gives 6376.5 N. Solving for the only unknown variable gives FD equals to 1617.87 N. For the rate of climb, it depends on the available excess power of the aircraft. In the case of the Borey aircraft, it has a maximum power of 73.5 kW. So, in case of the climb phase, if the current power used is 60 kW and the mass is 600 kg, the maximum power will be subtracted from the current power usage, and then divided by the weight, all in SI units. In this case, it will be 13500 W divided by 5886 N, which would equal to 2.29 m/s of climb. Calculating the rate of climb with different variables than the previous climb calculation, for take-off would be as follows; the velocity would be 23 m/s and the angle of attack would be 12°. Inserting those values will bring a climb rate of 4.78 m/s.

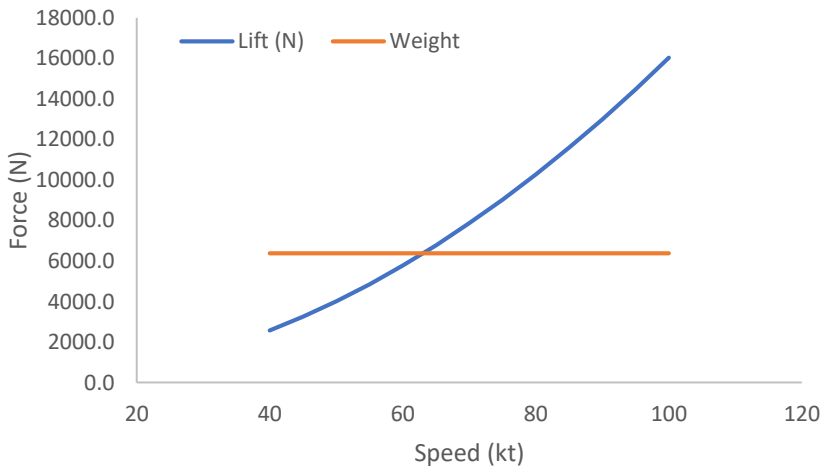

Figure 12: Weight and lift versus speed at AoA of 0° and 1,000 ft altitude

To determine the mass airflow, the propeller blade area, velocity and air density were considered. With a propeller diameter of 1.8 m, the area was calculated to be 2.54 m^2. Using an air density of 1.225 kg/m^3 and aircraft velocity of 23 m/s, mass airflow was found to be 71.56 kg/hr. The Borey aircraft's range variables is accounting for the maximum L/D, minimal specific fuel consumption (SFC) and the highest possible ratio of maximum weight to empty weight. This yielded a range of 720.6 km, closely aligning with the official performance figures.

Take-off

For take-off at maximum payload, the engine requires 5800 RPM, corresponding to 100 hp or 73.5 kW of output. Multiplying this power by specific fuel consumption (SFC) of 285 g/kW.hr (from regression analysis) results in a fuel burn rate of 20,520 g/hr. Using fuel density of 720 g/l, this translates to a fuel burn of 28.5 l/hr, which differs by 1.5 l/hr from the value in Table 3.

Table 3: Engine fuel consumption

Fuel consumption	Model: 912 S/ULS
At take-off performance	27.0 l/h (7.1 gal/hr)
At maximum continuous performance	25.0 l/h (6.6 gal/hr)
At 75 % continuous performance	18.5 l/h (4.9 gal/hr)
Specific consumption at maximum continuous performance	285 g/kW.hr (0.47 lb/hp.hr)

Climb

During climb, the aircraft operates with a 6° angle of attack and an engine RPM of no more than 5500. With power output of 70 kW and SFC of 255 g/kW.hr, the fuel burn rate is 24.79 l/hr, differing from the manufacturer's figure by 0.21 l/hr.

Cruising

Recommended cruise speeds are 70, 75 and 80 knots, requiring 4200, 4500 and 4700 RPM, respectively. At 80 knots with 4700 RPM, the engine output is 65 kW with SFC of 190 g/kW.hr, yielding a fuel burn of 12,350 g/hr. Dividing by the fuel density, this results in 17.15 l/hr, differing by 2.85 l/hr from the manufacturer's data.

Landing

Landing procedures use 6° angle of attack with a reduced engine power output of 45 kW, corresponding to an SFC of 100 g/kW.hr. This produces a fuel burn rate of 4500 g/hr, or 6.25 l/hr, which is 0.75 l/hr lower than the manufacturer's figure of 7 l/hr.

No Payload Fuel Burn

For the no-payload condition with a weight of 500 kg, the detailed fuel burn values for each segment are summarized in Table 4.

Table 4: Fuel burn with no payload

Flight Phase	Fuel Burn l/hr
Take-Off	21.92
Climb	19.07
Cruise	13.19
Descent	4.81

3.2 Mission performance

During take-off, fuel consumption was highest at approximately 27 l/hr, reflecting on the increased power demands. During cruise at 75% power, the fuel burn rate stabilized at 18.5 l/hr, offering an efficient range balance between fuel use and performance. Figure 13 and Figure 14 display the altitude versus time graphs for two missions, one covering 207 km and the other 720 km. These graphs highlight the fuel burn patterns across each flight phase, with steeper fuel usage during ascent phases and lower consumption during steady cruise segments. By analyzing these consumption patterns, the simulation revealed the Borey aircraft's operational efficiency under both full and partial payload conditions.

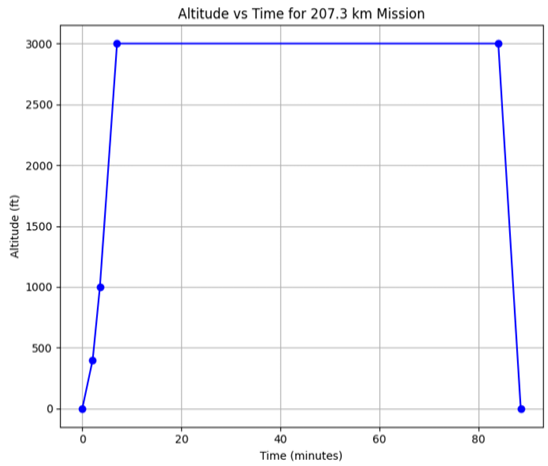

Figure 13: Altitude vs Time for Mission 1

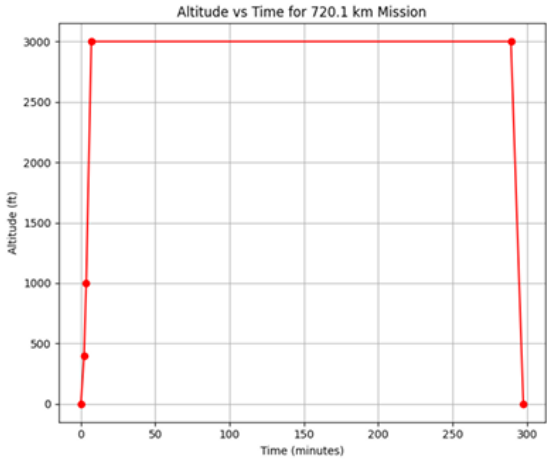

Figure 14: Altitude vs Time for Mission 2

The maximum range of the Borey aircraft was calculated using the Breguet Range Equation with the previously gathered aerodynamic data, which gave an estimated theoretical maximum range of 740 km. This range estimation also factored in optimal lift-to-drag ratios, propeller efficiency and specific fuel consumption rates, indicating the suitability of the Borey aircraft for medium-range missions. In addition, the comparison between no-payload and maximum-payload scenarios showed variations in range, with payload weight affecting the fuel burn rates and the overall efficiency. The payload analysis demonstrated that carrying the additional weight reduced the range due to increased fuel consumption, particularly during take-off and climb phases. This insight underscores the importance of balancing the payloads and fuel for the optimal mission planning, as heavier payloads will reduce the effective range, impacting mission flexibility for longer flights. Table 5 shows that, with a 20-liter fuel reserve out of the 90-liter usable fuel tank, the scenario in which there is no payload could perform the mission without tapping into the fuel reserves. Unlike the first case, the second scenario exceeds the 70 kg of operational fuel and it uses 10.15 kg extra of fuel that would be for the reserve fuel.

Table 5: Fuel consumption for Mission 2

Flight Phase	No Payload Fuel Burn (kg)	Maximum Payload Fuel Burn (kg)
Take-Off	0.7672	0.9975
First Climb	0.463	0.55
Second Climb	1.096	1.425
Cruise	66.825	80.708
Descent	0.668	0.868
Total	69.82	84.54

By inserting the weight values of this specific mission, the values of range in cruise can be calculated using the Breguet Range Equation. In this case, for maximum payload and maximum fuel, the estimated range was found to be 128.7 km. On the other hand, for no payload and maximum payload, the range was estimated to be 685.9 km. By using linear interpolation with these two calculated points, Figure 15 depicts the resultant payload-range trade-off plot.

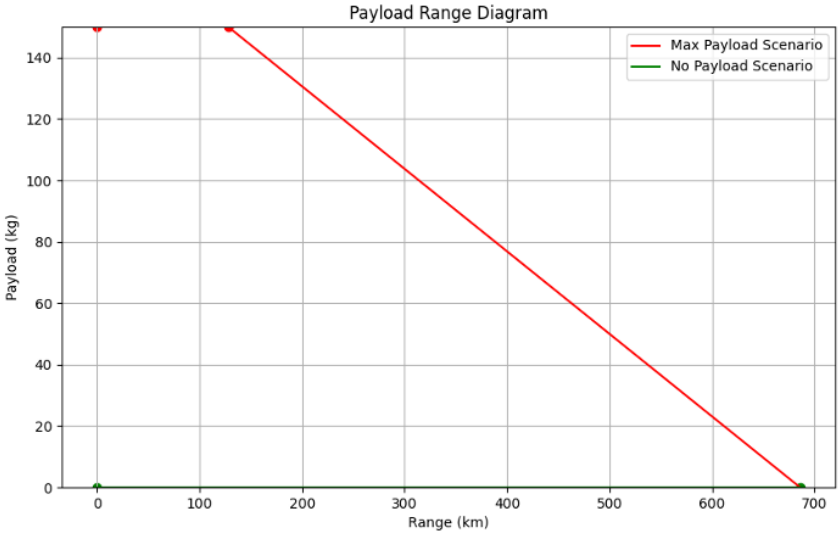

Figure 15: Payload-range plot

The results obtained for the Borey seaplane align well with the established aerodynamic principles observed in similar seaplanes. Studies such as those by Frant et al. (2021) on the float-equipped aircraft have indicated that seaplanes face higher drag coefficients due to floats, which reduce overall efficiency during cruise phases. The Borey aircraft's optimal L/D ratio at low angles of attack essentially reflects these aerodynamic trade-offs and underscores the design focus on maintaining efficiency at moderate speeds. Furthermore, the waypoint-based mission analysis approach used in this study takes inspiration from techniques commonly applied in UAV and small aircraft studies, allowing for detailed assessments of fuel burn and range [8]-[9]. Although there were relatively small differences in the results such as the range and fuel burn, the obtained results from this study were not significantly deviated from the aircraft manufacturer data as seen in Figure 16.

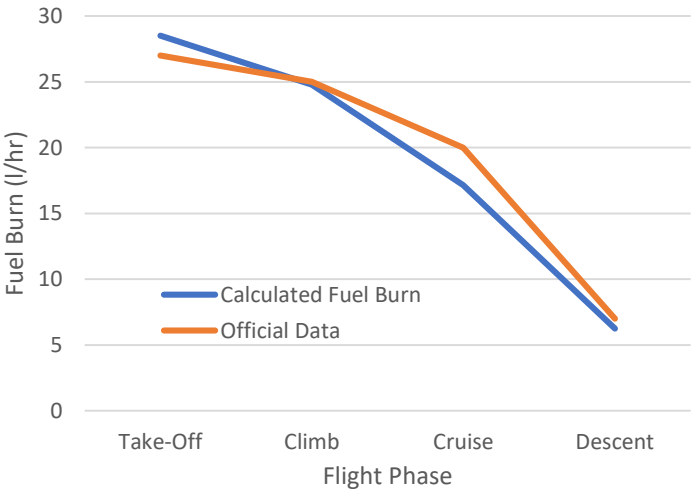

Figure 16: Calculated versus manufacturer's fuel burn data

3.3 Overall findings

The results from the wind tunnel testing and mission simulation provide a comprehensive view of the Borey seaplane's aerodynamic and mission performance characteristics. The data indicates that the Borey aircraft achieves its optimal L/D at a low angle of attack of around 3° and this condition is vital for maximizing efficiency during cruise flight. This peak L/D ratio of 8.9 aligns with the Borey aircraft's mission profile, which is mainly oriented towards steady, medium-range cruising rather than high-speed or highly dynamic maneuvers. The aerodynamic testing demonstrated that, as expected, drag increases significantly at higher angles of attack with a noticeable rise beyond 10°. This behavior limits the Borey aircraft's capability to operate efficiently at high angles, making it more suitable for low- and moderate-speed operations. This characteristic is ideal for a seaplane that needs to balance aerodynamic efficiency with additional drag forces encountered during take-off and landing on water. The mission performance simulation results further validate the Borey aircraft's design efficiency under realistic mission condition. Fuel burn rates were shown to stabilize during cruise phases, supporting the theoretical maximum range of 740 km calculated using the Breguet Range Equation. This range estimation was consistent with the aerodynamic data obtained from wind tunnel testing, confirming the model's reliability in representing the Borey aircraft's performance. However, the analysis also highlighted a reduction in range when the aircraft operates with maximum payload, emphasizing the importance of the payload management for optimizing mission efficiency.

The results obtained for the Borey seaplane align well with the established aerodynamic principles observed in similar seaplanes. Studies such as those by Kusuma et al [10] on the float-equipped aircraft have indicated that seaplanes face higher drag coefficients due to floats, which reduce overall efficiency during the cruise phases. The Borey aircraft's optimal L/D ratio at a low angle of attack reflects these aerodynamic trade-offs and underscores the design focus on maintaining efficiency at moderate speeds. Furthermore, the waypoint-based mission analysis approach used in this study mirrors the techniques commonly applied in unmanned aerial vehicle (UAV) and small aircraft studies, allowing for detailed phase-by-phase assessments of fuel burn and range. By segmenting the mission into specific waypoints, the simulation captures the unique demands placed on seaplanes, such as the fuel-intensive take-off and climb phases. This segmentation provides a granular view of the Borey aircraft's operational efficiency and reveals valuable insights into fuel-saving strategies during real-world missions.

The aerodynamic insights gained from this study offer important implications for the future design and the optimization of seaplanes. The high L/D ratio at a low angle of attack indicates that designs intended for efficient cruising would benefit from minimizing drag-inducing features. For the Borey aircraft, maintaining a lightweight structure and optimizing the hull design to reduce drag during water take-offs could further improve fuel efficiency, making the seaplane even more suitable for extended missions. The mission performance analysis also suggests that the seaplane designs could benefit from optimized fuel management systems that adapt to changes in payload and mission profile. By integrating more efficient propulsion systems or adjusting power output during non-cruise phases, designers could extend the range capabilities and reduce the operating costs. For the Borey aircraft, this could mean investigating hybrid or alternative powerplant options in future configurations, which might offer extra fuel savings and reduced environmental impact.

4. Conclusion and future work

This study successfully analyzed the aerodynamic and mission performance characteristics of the Borey seaplane, emphasizing its potential as an efficient, short-to-medium-range amphibious aircraft. The primary objectives, which include collecting the aerodynamic data through the wind tunnel testing, developing a simulation model and analyzing fuel burn across various flight phases, were met, providing

a detailed assessment of the seaplane's capabilities. The aerodynamic testing revealed that the Borey aircraft achieves an optimal L/D at low angles of attack, particularly favorable for cruise efficiency. This aligns well with the theoretical aerodynamic principles and also demonstrates the Borey aircraft 's design suitability for moderate-speed, efficient cruising. The mission performance analysis also underscored the Borey aircraft's range capabilities, showing that factors like payload weight significantly affect fuel consumption and range, especially during the fuel-intensive flight phases like takeoff and climb. The waypoint-based mission simulation provided insights into the fuel-saving strategies such as balancing payload with fuel to optimize range and highlighted potential design improvements for future seaplane models. These findings offer valuable implications for improving operational efficiency and they also lay a foundation for future studies in exploring alternative powerplant configurations such as hybrid-electric engines to enhance fuel efficiency and reduce emissions. Overall, this research contributes to the understanding of seaplane performance with practical applications for seaplane design and mission planning and provides a basis for exploring advanced propulsion technologies in amphibious aviation.

While this study provides valuable insights into the Borey seaplane's performance, there are several limitations that must be acknowledged. The 3D-printed model used for wind tunnel testing was scaled down, which may introduce scaling effects not present in a full-scale model. Scaling down an aircraft to 7.1% of its original size for wind tunnel testing introduces challenges such as Reynolds and Mach number mismatches, which affect boundary layer behavior. Surface roughness and also flow separation differ at smaller scales, leading to inaccuracies in drag and lift measurements. Structural deformations, propulsion interactions and wind tunnel wall interference further complicate results as these factors do not scale proportionally. Despite these limitations, techniques like corrections, precise manufacturing and sanding the surface of the model help to mitigate the discrepancies. Though every effort was made to ensure accuracy, the limitations of scaling mean that further studies with a full-scale model would be beneficial to fully validate the findings. This study did not account for real-world environmental factors such as wind turbulence or wave interactions, which are critical in shaping the performance of seaplanes. These factors can introduce additional drag, affect lift generation and influence stability, particularly during critical phases like take-off, landing and low-speed operations on water. Ignoring these variables may lead to an overly optimistic estimation of performance metrics such as range, fuel efficiency and operational reliability. Therefore, future work should also incorporate these environmental interactions to provide more accurate and practical assessment of the seaplane's capabilities. Additionally, the study was focused on the baseline ROTAX 912 ULS engine configuration and future work could explore the alternative power configurations such as hybrid-electric engines to evaluate potential improvements in fuel efficiency and environmental impact. Similarly, extending the waypoint-based mission simulation to incorporate varying environmental conditions such as wind or wave interaction during take-off and also landing on water could provide more robust view of the Borey aircraft's real-world operational capabilities. Finally, while the waypoint-based analysis was effective in modeling mission performance, further refinement of the simulation model to include real-time environmental changes could enhance the accuracy of the range and fuel consumption estimates. Future studies may also benefit from a more extensive dataset, incorporating a wider range of the operational conditions to fully capture the Borey aircraft's capabilities and limitations in diverse environments.

Acknowledgement

The authors thank Delta Industrial Sdn. Bhd. for providing the data for the Borey aircraft.

References

[1] AeroVolga. (2022). Borey: Designed for Wilderness. Retrieved from www.aerovolga.com/uploads/files/brochure-borey-web-13-01-2022.pdf

[2] A. Utomo, Gunawan and Yanuar, 'Biomimetics Design Optimization and Drag Reduction Analysis for Indonesia N219 Seaplanes Catamaran Float', Processes, vol. 9, no. 11, 2021.

[3] S. Wang, Z. Li and Q. Zhang, 'An Energy Efficiency Optimization Method for Electric Propulsion Units during Electric Seaplanes' Take-Off Phase', Aerospace, vol. 11, no. 2, 2024.

[4] N. Shabrina, D. Arianto, K. S. Wardani, Z. Qonita, A. R. Ispandiari, N. I. Gutami and M. F. Manti, 'Session Assessment of Seaplane Operations: The Case of Marine Tourism Development on Gili Iyang Island, Indonesia', IOP Conference Series: Earth and Environmental Science, vol. 1166, no. 1, 2023.

[5] X. Roboam, 'A Review of Powertrain Electrification for Greener Aircraft', Energies, vol. 16, no. 19, 2023.

[6] Delta Aerospace. (2024). Delta Aerospace. Retrieved from https://www.deltaaerospace.org

[7] ROTAX. (2019). Operators Manual for ROTAX Engine Type 912 Series. Retrieved from https://www.rotax-owner.com/manuals/OM_912iSeries_ED2_R1.pdf

[8] L. M. Silverberg and D. Xu, 'Dubins Waypoint Navigation of Small-Class Unmanned Aerial Vehicles', Open Journal of Optimization, vol. 8, no. 2, 2019.

[9] S. He, H.-S. Shin, A. Tsourdos and C.-H. Lee, 'Energy-Optimal Waypoint-Following Guidance Considering Autopilot Dynamics', IEEE Transactions on Aerospace and Electronic Systems, vol. 56, no. 4, pp. 2701-2717, 2020.

[10] Y. F. Kusuma, H. Sulistiya, B. H. Muhammad, I. Ansori, A. D. Kurniawan, G. Verma, D. H. Priatno, A. P. Fuadi, S. Syamsuar and W. Karyawan, 'The Effect of Floater Shape on Amphibious Aircraft's Drag Coefficient Using Computational Fluid Dynamics Method', International Review of Aerospace Engineering, vol. 17, no. 2, 2024.


eISSN 3009-0520
9 773009 052004